ChemPubSoc Europe

DOI: 10.1002/chem.201404988

CHEMISTRY
A European Journal
Communication

Enzyme Models |*Hot Paper*|

# Experimental and Computational Evidence for the Mechanism of Intradiol Catechol Dioxygenation by Non-Heme Iron(III) Complexes

Robin Jastrzebski,[a, b] Matthew G. Quesne,[b] Bert M. Weckhuysen,[a] Sam P. de Visser,*[b] and Pieter C. A. Bruijnincx*[a]

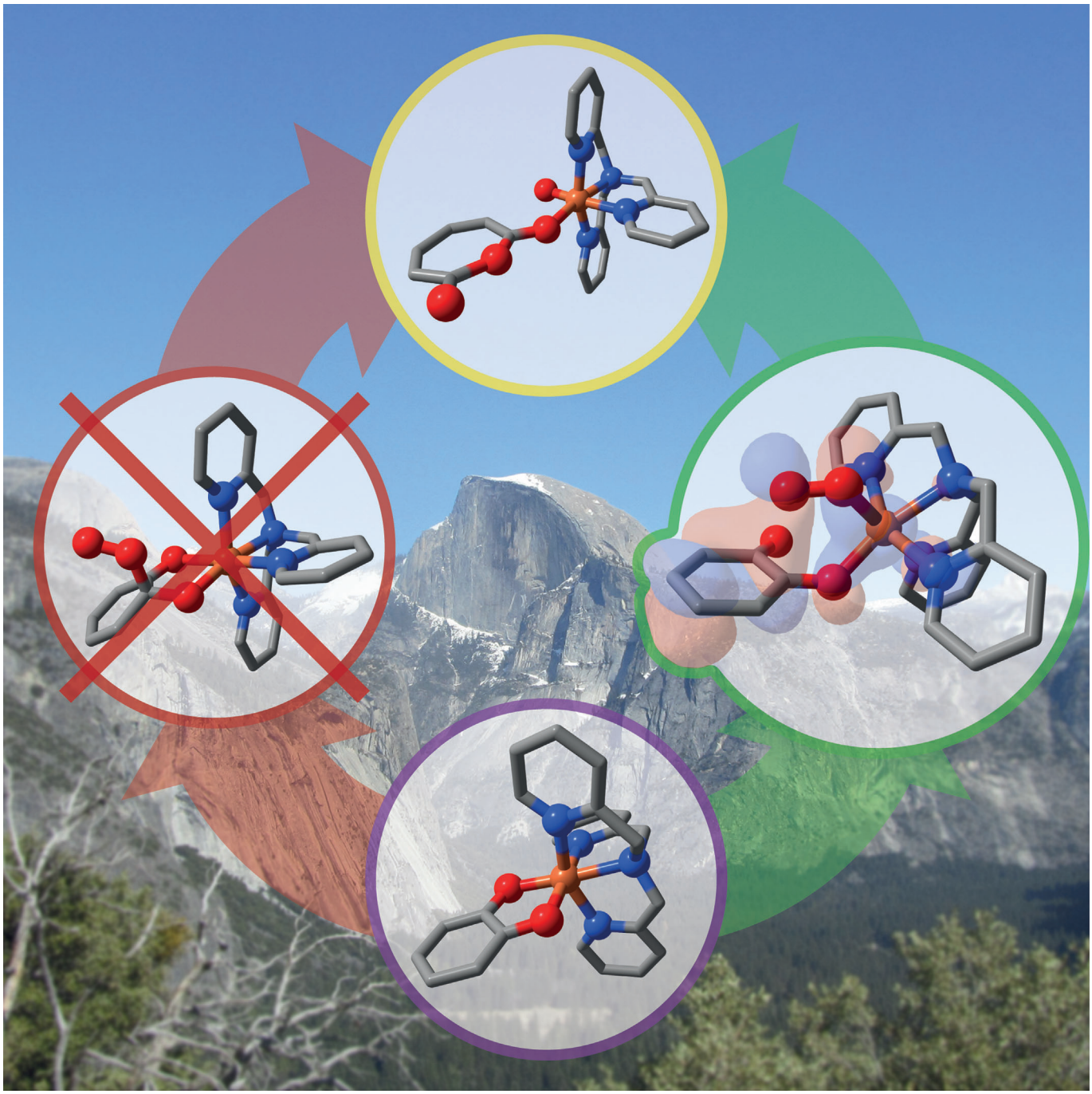

 

**Abstract:** Catechol intradiol dioxygenation is a unique reaction catalyzed by iron-dependent enzymes and non-heme iron(III) complexes. The mechanism by which these systems activate dioxygen in this important metabolic process remains controversial. Using a combination of kinetic measurements and computational modelling of multiple iron(III) catecholato complexes, we have elucidated the catechol cleavage mechanism and show that oxygen binds the iron center by partial dissociation of the substrate from the iron complex. The iron(III) superoxide complex that is formed subsequently attacks the carbon atom of the substrate by a rate-determining C–O bond formation step.

Enzymatic oxidation of catechols is a key step in catabolic pathways for the decomposition of aromatic substrates. Three classes of enzymes are known: catechol oxidases oxidize the substrate to the corresponding quinone in a two-electron process at a copper active site. Extradiol dioxygenases feature an iron(II) active site and insert molecular oxygen adjacent to the hydroxyl functionalities to afford muconic semialdehydes. Intradiol dioxygenases, finally, cleave the C–C bond between the two hydroxyl functionalities of catecholic substrates, to yield derivatives of *cis,cis*-muconic acid.[1] The latter reaction has been shown to proceed at a mononuclear iron(III) center with molecular oxygen as the oxidant.[2] Bio-inspired iron(III) complexes featuring various tetradentate donor ligands, of which tris(2-pyridylmethyl)amine (TPA) is the most active, were also found capable of selective intradiol catechol dioxygenation.[3] Such systems do not only provide additional insight into the enzymatic processes, but are also useful for the biodegradation of (chlorinated) aromatic compounds[4] and may provide a sustainable, catalytic route for the production of the nylon feedstock adipic acid.[5]

The catalytic mechanism of both the enzymes and biomimetic compounds is currently surrounded by major controversies due the fact that most oxygen-bound intermediates have a short lifetime and have not been trapped or characterized experimentally. Currently, two proposed mechanisms seem to support experimental product distributions and isotope effects: dioxygen can attack the substrate directly and subsequently react by a Criegee rearrangement or, alternatively, bind the iron(III) center prior to substrate attack and O–O bond homolysis.[6]

The 'substrate activation' mechanism was first proposed by Que et al.[3a,7] to explain the reactivity of (coordinatively saturated) catecholato complexes towards oxygen. A partial reduction of the catecholate to a semiquinone radical was suggested to enable direct electrophilic attack by oxygen on the substrate (pathway a in Scheme 1). Such a mechanism would explain the persistence of the iron(III) state during reaction that is seen by EPR and accounts for the observation that even coordinatively saturated bio-inspired complexes show oxidative cleavage activity. Interestingly, the enzyme (1*H*)-3-hydroxy-4-oxoquinaldine 2,4-dioxygenase catalyzes intradiol dioxygenation without the use of a transition-metal co-factor by direct attack of molecular oxygen on the substrate,[8] which would support a mechanism analogous to pathway a. However, more recently an 'oxygen activation' mechanism has been proposed,[9] wherein oxygen must first bind to the iron(III) center instead (pathway b in Scheme 1). Better understanding of this key mechanistic step and the function of the metal center in catalysis will improve our understanding of the enzymatic reactions and allow for the development of more active bio-inspired systems. This encouraged us to do a detailed combined experimental and computational study, which provides evidence that oxygen binds the iron center prior to substrate activation and that the rate-determining step involves C–O bond formation.

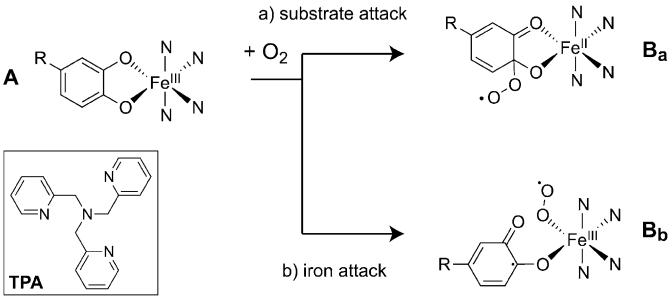


**Scheme 1.** Key mechanistic possibilities of oxygen attack on an iron(III)–catecholato complex leading to intradiol dioxygenation.

To elucidate the catalytic mechanism and, in particular, the nature of the dioxygen binding step, we performed kinetic measurements for stoichiometric intradiol dioxygenation by in situ prepared iron(III) complexes. Pseudo first-order rate constants (Supporting Information, Table S1) could be conveniently obtained by monitoring the decay of the catecholate-to-iron charge-transfer band at approximately 800 nm (Figure 1a). Iron complexes were prepared with TPA and the novel TPA-derivative tris(4-chloro-2-pyridylmethyl)amine ($Cl_3$-TPA) and *p*-substituted catechols. As also previously observed, complexes of more electron-donating catechols and more electron-withdrawing ligands were more active.[3b,9]

[a] *R. Jastrzebski, Prof. Dr. B. M. Weckhuysen, Dr. P. C. A. Bruijnincx*
*Inorganic Chemistry and Catalysis*
*Debye Institute for Nanomaterials Science*
*Utrecht University, Universiteitsweg 99*
*3584 CG Utrecht (The Netherlands)*
*E-mail: p.c.a.bruijnincx@uu.nl*

[b] *R. Jastrzebski, Dr. M. G. Quesne, Dr. S. P. de Visser*
*The Manchester Institute for Biotechnology and the*
*School of Chemical Engineering and Analytical Science*
*The University of Manchester*
*131 Princess Street, Manchester, M1 7DN (UK)*
*E-mail: sam.devisser@manchester.ac.uk*

*Supporting information for this article is available on the WWW under http://dx.doi.org/10.1002/chem.201404988.*

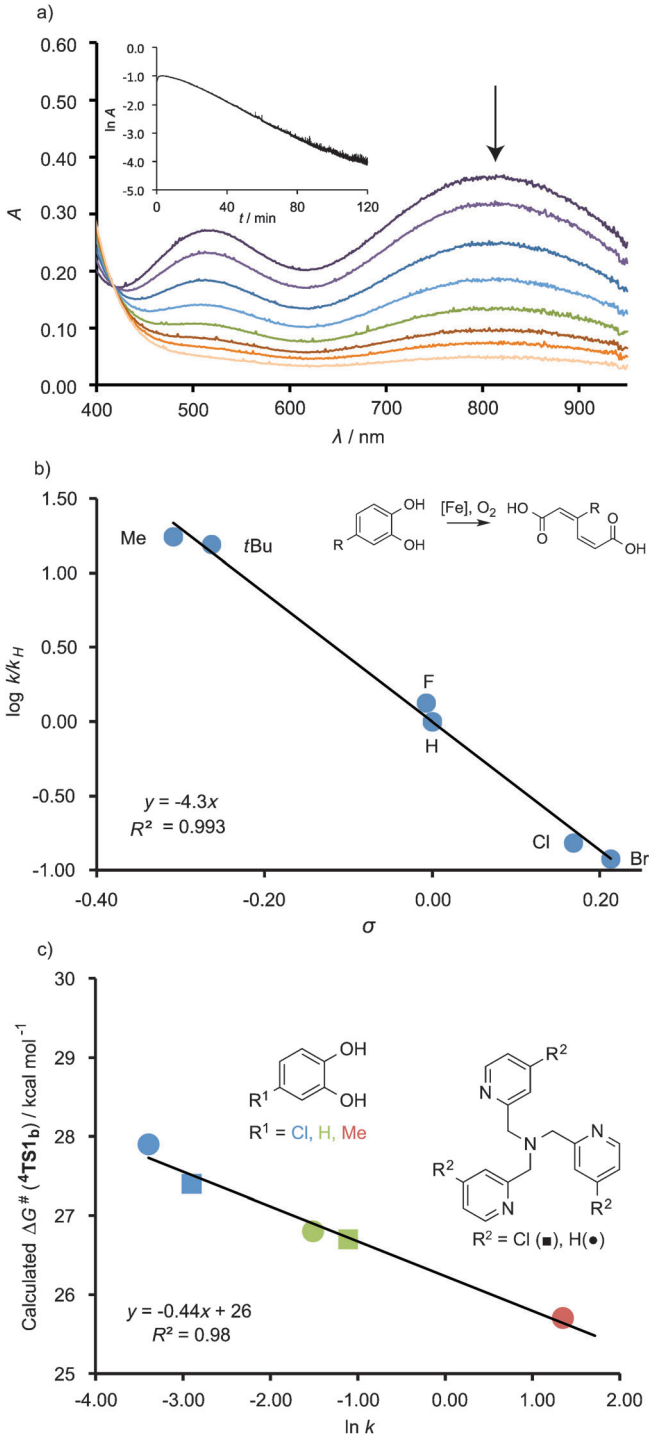


**Figure 1.** a) UV/Vis spectra of the iron(III) TPA catecholato complex, showing decreasing intensity of the charge-transfer bands in time (inset: ln A at 804 nm vs. time). b) Hammett plot for the rate of intradiol dioxygenation with different catechols by the iron(III) TPA complex, using the Swain–Lupton equation for a scaled field and resonance effect[11] ($\alpha = 1.14$). c) Excellent agreement is obtained between the natural logarithm of the experimentally determined rate constant and the calculated energy barrier.

A Hammett analysis of the rate data already provided initial mechanistic information (Figure 1b). As the reaction may proceed at the carbon atom *meta* or *para* to the substituent, fits were first attempted against both parameters $\sigma_m$ and $\sigma_p^+$,[10] with the latter giving a considerably better fit. The ambiguity of the *meta* and *para* positions in this system, however, requires scaling of the resonance and field components of the Hammett parameter using the Swain–Lupton parameters for *para* substituents.[10,11] An excellent fit is obtained with a value of $\alpha = 1.14$, indicating a slightly stronger inductive effect than expected for a pure *para* substituent. The strongly negative value of the reaction constant $\rho = -4.33$ indicates a transfer of negative charge away from the catecholate moiety in the rate-determining step, which implies that the rate-determining step involves an electrophilic attack of oxygen on the catecholate moiety. However, this information alone does not allow one to discriminate yet between pathways a and b.

To gain a better understanding of the mechanism of catechol intradiol dioxygenation by our iron(III) complexes we decided to run a set of density functional theory (DFT) calculations following methods previously tested and benchmarked on analogous systems.[12] Geometry optimization of the iron(III) catecholato complex ($^6$**A**) revealed carbon–oxygen bond lengths of 1.34 and 1.35 Å, which are consistent with the reported crystal structure coordinates.[13] The sextet spin state was found to be the electronic ground state at room temperature, with the doublet ($^2$**A**) state being more stable at 0 K. This is in excellent agreement with the experimentally observed spin-crossover behavior.[14] While there is significant spin density on the catecholate moiety (0.82), it is primarily located on the oxygen atoms, originating from a covalent interaction between the catecholate $\pi^*$ and iron $t_{2g}$ orbitals. Thus, based on the bond lengths and spin densities, the catecholate moiety does not appear to have the semiquinone character that is required for pathway *a*.

We then focused on the relative energies of oxygen adducts $\mathbf{B_a}$ and $\mathbf{B_b}$ (Scheme 1) and ran geometry optimizations for all low-lying spin states (i.e., doublet, quartet and sextet). Importantly, no stable local minimum could be found on any of the spin state surfaces for structure $\mathbf{B_a}$ as all attempts relaxed to structure **A** (and unbound oxygen) instead. A constrained geometry optimization with fixed C–O distance converged to a structure that was $>30$ kcal mol$^{-1}$ higher in energy than $^6$**A**. In addition to structure $\mathbf{B_b}$, we also considered a complex with the catecholate bound bidentately and TPA as a tridentate ligand ($\mathbf{B_b}'$). In the quartet spin state, both $\mathbf{B_b}$ and $\mathbf{B_b}'$ could be located and characterized as a high-spin iron(III) center anti-ferromagnetically coupled to a superoxide. As these states were found to be very close in free energy (within 1 kcal mol$^{-1}$), the activation barriers of C–O bond formation (**TS1**) leading to the peroxo-bridged intermediates **C**, were investigated for both, see Figure 2. Rather surprisingly, the transition state ($\Delta G^{\#}$ 26.8 vs. 39.2 kcal mol$^{-1}$) and peroxo intermediate ($\Delta G$ 19.9 vs. 30.0 kcal mol$^{-1}$) were both found to be considerably more favorable if the catecholate was dissociated. Peroxo-bridged intermediates analogous to **C** have been proposed before in the catalytic cycles of catechol dioxygenases and other non-heme iron enzymes[15] and may undergo O–O bond homolysis. We find that homolytic O–O bond cleavage can indeed proceed through transition state $^4$**TS2** (26.3 kcal mol$^{-1}$) to form radical intermediate ($^4$**D**) on the quartet spin state surface. The subse-

 

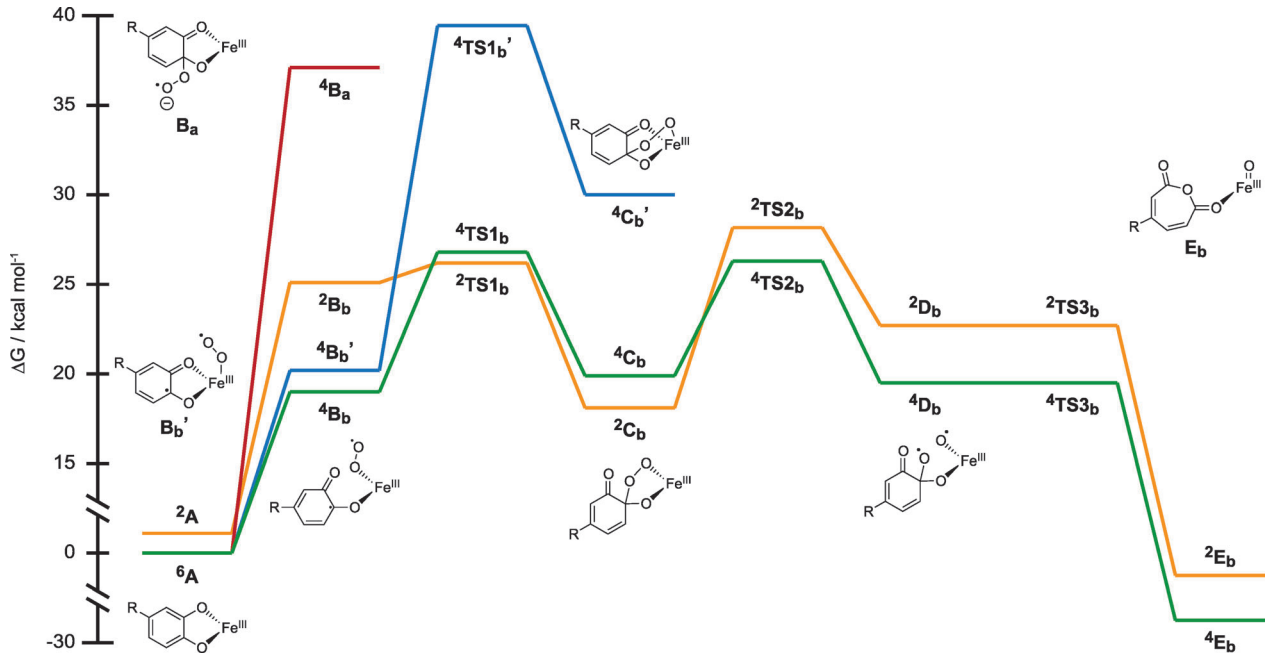


**Figure 2.** Free-energy landscape for the dioxygenation of catechol (R = H) by the iron(III) complex of TPA. The pathway with direct substrate attack by oxygen (red) was found to be inaccessible. Oxygen attack on the iron center was found to be more favorable if the substrate (quartet: green, doublet: yellow), rather than the ligand (blue), partially dissociated.

quent rearrangement to form the muconic anhydride product $^4$**E** via $^4$**TS3** then proceeds essentially barrierless.

A similar mechanism can also occur on the doublet spin state surface, although the total barrier is higher. Consequently, based on our computational results, the rate-determining step is predicted to involve $^4$**TS1** at 26.8 kcal mol$^{-1}$. Although this is somewhat high for the experimental rate constant of 0.2 M$^{-1}$ s$^{-1}$, it is likely that the entropic contribution for oxygen binding is systematically overestimated in our calculation. Having $^4$**TS1** as the rate-determining step nevertheless is in agreement with the experimental results from the Hammett analysis, as it involves the electrophilic attack of oxygen on the catecholate moiety. To test this hypothesis, we optimized the intermediates and transition states in the early part of the mechanism with other *p*-substituted catechols and/or TPA ligands. A comparison of the natural logarithm of the pseudo-first-order rate constants with the calculated barrier $^4$**TS1** shows an excellent correlation between the two (Figure 1c), suggesting that our proposed mechanism is indeed valid.

Intermediates $^4$**B**$_b$ and $^4$**C**$_b$ are key to improved understanding of the reactivity of the iron(III) catecholato complexes. Both intermediates retain a distorted octahedral coordination environment around the iron center, with the dissociated catecholate arm stabilized by hydrogen bonding to an adjacent pyridine donor. Oxygen is bound *trans* to a pyridine N-donor and already points at the reactive catecholate carbon in $^4$**B**$_b$ (C–O distance 2.505 Å). Interestingly, the catecholate moiety has been oxidized at this point to a semiquinone, as indicated by the shortening of one of the C–O bonds to 1.27 Å, the decrease in natural charge as well as the observation that spin density is located primarily on the carbon atoms. The charge distribution shows the oxidant to be not iron, but oxygen, which is reduced to a superoxide stabilized by σ-donation to the iron center. To accommodate this formally spin-forbidden reaction, the iron center acts as a buffer, accepting (down-spin) electron density from the catecholate in its $t_{2g}$-symmetry orbitals, while mixing up-spin density from the $e_g$ orbitals into the oxygen π*. Such a transfer mechanism has been previously proposed by Solomon et al. for the enzymatic mechanism.[16] As the semiquinone π and oxygen π* orbitals now both are singly occupied and have good overlap, the C–O bond can subsequently be formed by recombination of the anti-parallel electrons to obtain $^4$**C**$_b$. In line with the principal role of iron as an electron buffer, its spin state has changed from a sextet state in $^6$**A** to a quartet state in $^4$**C**$_b$. The electron-transfer mechanism is schematically depicted in Figure 3.

Given the mechanism proposed, the influence of the substrate on reactivity can be clearly understood in terms of the energy level of the frontier catecholate π orbital, facilitating electron transfer away from the more electron-rich substrates. The influence of the ligand on the cleavage rate has, on the other hand, often been linked to the iron center's Lewis acidity[3,4a] for which the $\lambda_{max}$ of the CT bands of the catecholato complexes were taken as a measure.[17] However, based on our mechanism the net electron transfer to or from iron is actually quite limited. Instead, the ligand field must be able to stabilize the quartet spin state to facilitate the oxidation of the catechol moiety by oxygen. Indeed, the symmetry of the TPA ligand is such that π-backbonding with all three pyridine donors involves only a single $t_{2g}$ orbital, consequently lowering the energy of the quartet state. This increased backbonding is clearly strongest in the pyridine donor *trans* to oxygen, for

 

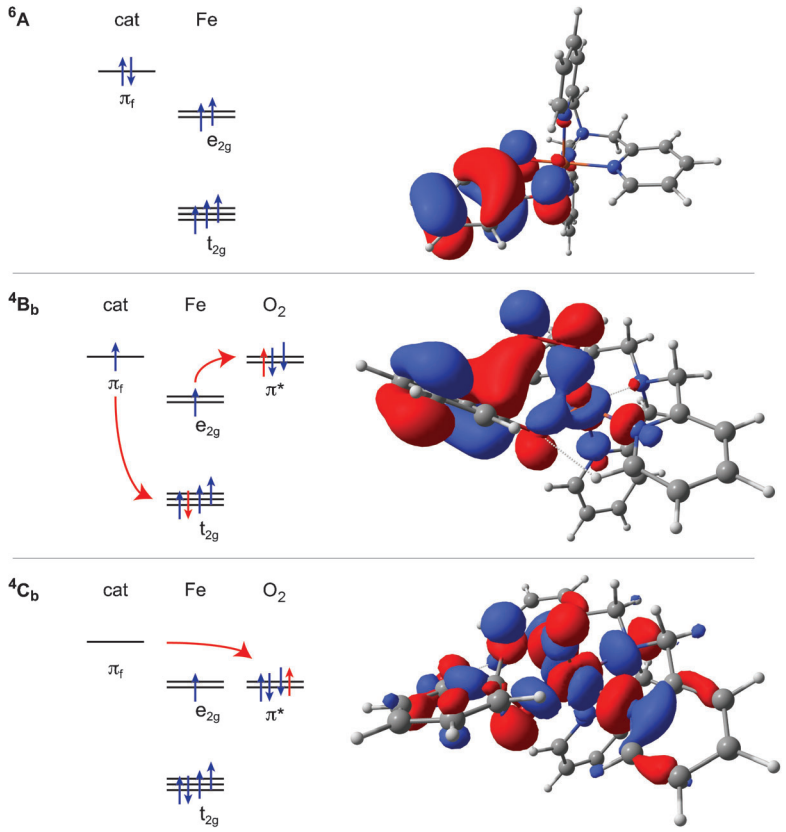


**Figure 3.** Simplified orbital diagrams of the states $^6$**A**, $^4$**B**$_b$ and $^4$**C**$_b$. Red arrows indicate the electron transfers involved in their formation. Isosurfaces of the up-spin HOMOs are shown on the right.

which the Fe–N bond distance decreases from 2.14 to 2.00 going from $^6$**A** to $^4$**C**$_b$. As this backbonding interaction will be stronger for more electron-withdrawing ligands, the previously noted relationship between Lewis acidity of the iron center and activity holds only for sets of ligands that have the same symmetry.[18] Thus, our results also provide insight into why ligands, such as bispicen and bispidine, which at first sight might have electronic properties that seem well-suited for the reaction, show little intradiol dioxygenation activity (see Figure S6 in the Supporting Information).[19] As evident from the crystal structures of the iron-catecholate complexes of these ligands (Figure S6 in the Supporting Information), oxygen must bind *trans* to an aliphatic amine, if a similar mechanism is active. These aliphatic amine donors are clearly worse ligands in terms of backbonding and in this geometry are unable to stabilize the quartet state. Furthermore, with bispicen[19a] the two pyridine donors positioned *cis* to oxygen have their rings rotated 90° with respect to each other, and as a result the interaction with iron will involve two separate $t_{2g}$ orbitals, further reducing the stability of the quartet state. This interpretation is further supported by an azocyclic system[18a] (see Figure S6c in the Supporting Information) that shares the same N-donor functionalities, but reacts two orders of magnitude faster. In this system, oxygen must bind *trans* to one of the pyridine donors, and the pyridine donors have the correct symmetry for interacting with a single $t_{2g}$ orbital, enabling better stabilization of the quartet state. Other peculiar features that have been previously observed in intradiol dioxygenation by non-heme iron(III) complexes can also now be better understood based on our mechanistic results. For instance, if both *N*-methyl groups in the azocyclic system were replaced by hydrogen atoms,[20] its reactivity increased by two orders of magnitude. The increase in activity can now be attributed to more facile catechol dissociation, as the free N–H groups are significantly better hydrogen-bond donors than the pyridine hydrogens in TPA. The influence of the ease of catechol dissociation is also evident from the unusually low reactivity of 3,6-di-*tert*-butylcatechol towards dioxygenation by the iron(III) TPA complex. Presumably, the bulky *tert*-butyl groups hinder the rotation of the catecholate moiety that is necessary to enable oxygen binding.[9a]

Given that the electron-transfer mechanism found here is very much in agreement with the one previously suggested by Solomon et al.[16] for the enzymatic system, it seems likely that there are important similarities in the enzymatic and biomimetic mechanisms, despite the obvious structural differences. As in our work, geometry optimization on a small model of the enzyme–substrate–oxygen adduct did yield two $^4$**C**$_b$-like intermediates, with partially dissociated catecholates. The obtained ligand fields were square-pyramidal rather than octahedral, which would also assist in stabilization of the quartet state. A previous hydrid DFT study on protocatechuate 3,4-dioxygenase[15a] reported an oxygen-bound intermediate very similar to $^4$**B**$_b$′ (i.e. a superoxide with catechol bound as a dianion) and a subsequent high barrier for bridging peroxide formation, as in this work. To obtain a reasonable barrier, a spin-crossover to the sextet state was proposed. However, as iron still had a free coordination site for oxygen, a mechanism wherein catechol dissociates was not considered. The importance of the second-shell residues for the reactivity in the native enzymes has been well-documented[15a,21] and stabilization of the dissociated catecholate in a $^4$**B**$_b$-like intermediate may well be facilitated by strong hydrogen bonding with for example, Arg-221 in 1,2-catechol dioxygenase.[22] Finally, we note that the barrier for subsequent homolytic cleavage was found to be only 0.5 kcal mol$^{-1}$ lower than carbon–oxygen bond formation, which we find rate-determining. To obtain substantially more reactive systems, it is therefore necessary to address both steps, which is challenging as they have contrasting electronic requirements. This appears to be elegantly solved by the enzyme as

 

a tyrosine ligand, which dissociates upon substrate binding, is thought to recoordinate further down the catalytic cycle.[15b] If this occurs after the bridging peroxide formation, a more electron-rich iron center is formed, facilitating the subsequent homolytic cleavage. These features will need to be further investigated in the actual enzymatic systems to confirm this hypothesis.

In conclusion, experimental rate data combined with DFT results allowed us to discriminate between proposed mechanisms for catechol intradiol dioxygenation by non-heme iron(III) complexes with TPA-derived ligands. Based on our results, oxygen first coordinates to the ferric center at a vacant site generated by partial dissociation of the catecholate substrate, which is simultaneously oxidized to a semiquinone by oxygen, with the iron center acting as an electron buffer. The subsequent carbon–oxygen bond formation is then rate-determining. The mechanism provides a good explanation for both the effect of substrate and ligand electronic structure on reactivity. Undoubtedly the mechanistic insight provided will assist in the design of more active catechol intradiol dioxygenation mimics.

## Acknowledgements

P.C.A.B. acknowledges the Netherlands Organization for Scientific Research (NWO) for a Vernieuwingsimpuls Veni Grant. M.G.Q. thanks the BBSRC for a studentship. The CSF at the University of Manchester and the National Service of Computational Chemistry Software are acknowledged for computational resources to S.P.d.V.

**Keywords:** biomimetic models · density functional theory · enzyme models · kinetics · reactivity

[1] a) T. D. H. Bugg, *Tetrahedron* **2003**, *59*, 7075 – 7101; b) M. Costas, M. P. Mehn, M. P. Jensen, L. Que Jr., *Chem. Rev.* **2004**, *104*, 939 – 986; c) F. H. Vaillancourt, J. T. Bolin, L. D. Eltis, *Crit. Rev. Biochem. Mol. Biol.* **2006**, *41*, 241 – 267; d) S. P. de Visser, D. Kumar, (Eds.) *Iron-containing enzymes: Versatile catalysts of hydroxylation reaction in nature*. RSC Publishing, Cambridge (UK), **2011**.

[2] a) O. Hayaishi, M. Katagiri, S. Rothberg, *J. Am. Chem. Soc.* **1955**, *77*, 5450 – 5451; b) D. H. Ohlendorf, J. D. Lipscomb, P. C. Weber, *Nature* **1988**, *336*, 403 – 405; c) E. I. Solomon, T. C. Brunold, M. I. Davis, J. N. Kemsley, S.-K. Lee, N. Lehnert, F. Neese, A. J. Skulan, Y.-S. Yang, J. Zhou, *Chem. Rev.* **2000**, *100*, 235 – 350.

[3] a) H. G. Jang, D. D. Cox, L. Que Jr., *J. Am. Chem. Soc.* **1991**, *113*, 9200 – 9204; b) R. Yamahara, S. Ogo, H. Masuda, Y. Watanabe, *J. Inorg. Biochem.* **2002**, *88*, 284 – 294; c) P. C. A. Bruijnincx, G. van Koten, R. J. M. Klein Gebbink, *Chem. Soc. Rev.* **2008**, *37*, 2716 – 2744.

[4] a) T. Funabiki, T. Yamazaki, A. Fukui, T. Tanaka, S. Yoshida, *Angew. Chem. Int. Ed.* **1998**, *37*, 513 – 515; *Angew. Chem.* **1998**, *110*, 527 – 530; b) A. Alfreider, C. Vogt, W. Babel, *Appl. Environ. Microbiol.* **2003**, *69*, 1372 – 1376.

[5] R. Jastrzebski, B. M. Weckhuysen, P. C. A. Bruijnincx, *Chem. Commun.* **2013**, *49*, 6912 – 6914.

[6] T. D. H. Bugg, Chapter 2 in Reference 1d.

[7] D. D. Cox, L. Que Jr., *J. Am. Chem. Soc.* **1988**, *110*, 8085 – 8092.

[8] A. Hernandez-Ortega, M. G. Quesne, S. Bui, D. P. H. M. Heuts, R. A. Steiner, D. J. Heyes, S. P. de Visser, N. S. Scrutton, *J. Biol. Chem.* **2014**, *289*, 8620 – 8632.

[9] a) Y. Hitomi, M. Yoshida, M. Higuchi, H. Minami, T. Tanaka, T. Funabiki, *J. Inorg. Biochem.* **2005**, *99*, 755 – 763; b) M. Higuchi, Y. Hitomi, H. Minami, T. Tanaka, T. Funabiki, *Inorg. Chem.* **2005**, *44*, 8810 – 8821.

[10] C. Hansch, A. Leo, R. W. Taft, *Chem. Rev.* **2002**, *102*, 783.

[11] C. G. Swain, E. C. Lupton, *J. Am. Chem. Soc.* **1968**, *90*, 4328 – 4337.

[12] a) R. Latifi, M. A. Sainna, E. V. Rybak-Akimova, S. P. de Visser, *Chem. Eur. J.* **2013**, *19*, 4058 – 4068; b) M. G. Quesne, R. Latifi, L. E. Gonzalez-Ovalle, D. Kumar, S. P. de Visser, *Chem. Eur. J.* **2014**, *20*, 435 – 446.

[13] A. J. Simaan, M.-L. Boillot, R. Carrasco, J. Cano, J.-J. Girerd, T. A. Mattioli, J. Ensling, H. Spiering, P. Gütlich, *Chem. Eur. J.* **2005**, *11*, 1779 – 1793.

[14] A. J. Simaan, M.-L. Boillot, E. Rivière, A. Boussac, J.-J. Girerd, *Angew. Chem. Int. Ed.* **2000**, *39*, 196 – 198; *Angew. Chem.* **2000**, *112*, 202 – 204.

[15] a) T. Borowski, P. E. M. Siegbahn, *J. Am. Chem. Soc.* **2006**, *128*, 12941 – 12953; b) M. Xin, T. D. H. Bugg, *J. Am. Chem. Soc.* **2008**, *130*, 10422 – 10430.

[16] M. Y. M. Pau, M. I. Davis, A. M. Orville, J. D. Lipscomb, E. I. Solomon, *J. Am. Chem. Soc.* **2007**, *129*, 1944 – 1958.

[17] D. D. Cox, S. J. Benkovic, L. M. Bloom, F. C. Bradley, M. J. Nelson, L. Que Jr., D. E. Wallick, *J. Am. Chem. Soc.* **1988**, *110*, 2026 – 2032.

[18] a) W. O. Koch, H.-J. Krüger, *Angew. Chem. Int. Ed. Engl.* **1995**, *34*, 2671 – 2674; *Angew. Chem.* **1995**, *107*, 2928 – 2931; b) M. Pascaly, M. Duda, F. Schweppe, K. Zurlinden, F. K. Müller, B. Krebs, *J. Chem. Soc. Dalton Trans.* **2001**, 828 – 837.

[19] a) P. Mialane, L. Tchertanov, F. Banse, J. Sainton, J.-J. Girerd, *Inorg. Chem.* **2000**, *39*, 2440 – 2444; b) P. Comba, H. Wadepohl, S. Wunderlich, *Eur. J. Inorg. Chem.* **2011**, *2011*, 5242 – 5249.

[20] N. Raffard, R. Carina, A. J. Simaan, J. Sainton, E. Rivière, L. Tchertanov, S. Bourcier, G. Bouchoux, M. Delroisse, F. Banse, J. Girerd, *Eur. J. Inorg. Chem.* **2001**, *2001*, 2249 – 2254.

[21] P. C. A. Bruijnincx, M. Lutz, A. L. Spek, W. R. Hagen, G. van Koten, R. J. M. Klein Gebbink, *Inorg. Chem.* **2007**, *46*, 8391 – 8402.

[22] M. W. Vetting, D. H. Ohlendorf, *Structure* **2000**, *8*, 429 – 440.

Received: August 25, 2014
Published online on October 16, 2014

 